Electronic Supplementary Material (ESI) for Chemical Science.
This journal is © The Royal Society of Chemistry 2014

Electronic Supporting Information

NMR and TRLFS Studies of Ln(III) and An(III) C5-BPP Complexes†

Christian Adam,*[a,b] Björn B. Beele,[a,b] Andreas Geist,[a] Udo Müllich,[a] Peter Kaden,[a] and Petra J. Panak[a,b]

[a] Karlsruhe Institute of Technology (KIT), Institute for Nuclear Waste Disposal (INE), P.O. Box 3640, 76021 Karlsruhe, Germany

[b] University of Heidelberg, Institute for Physical Chemistry, Im Neuenheimer Feld 253, 69120 Heidelberg, Germany.

Contents

Mass Spectra

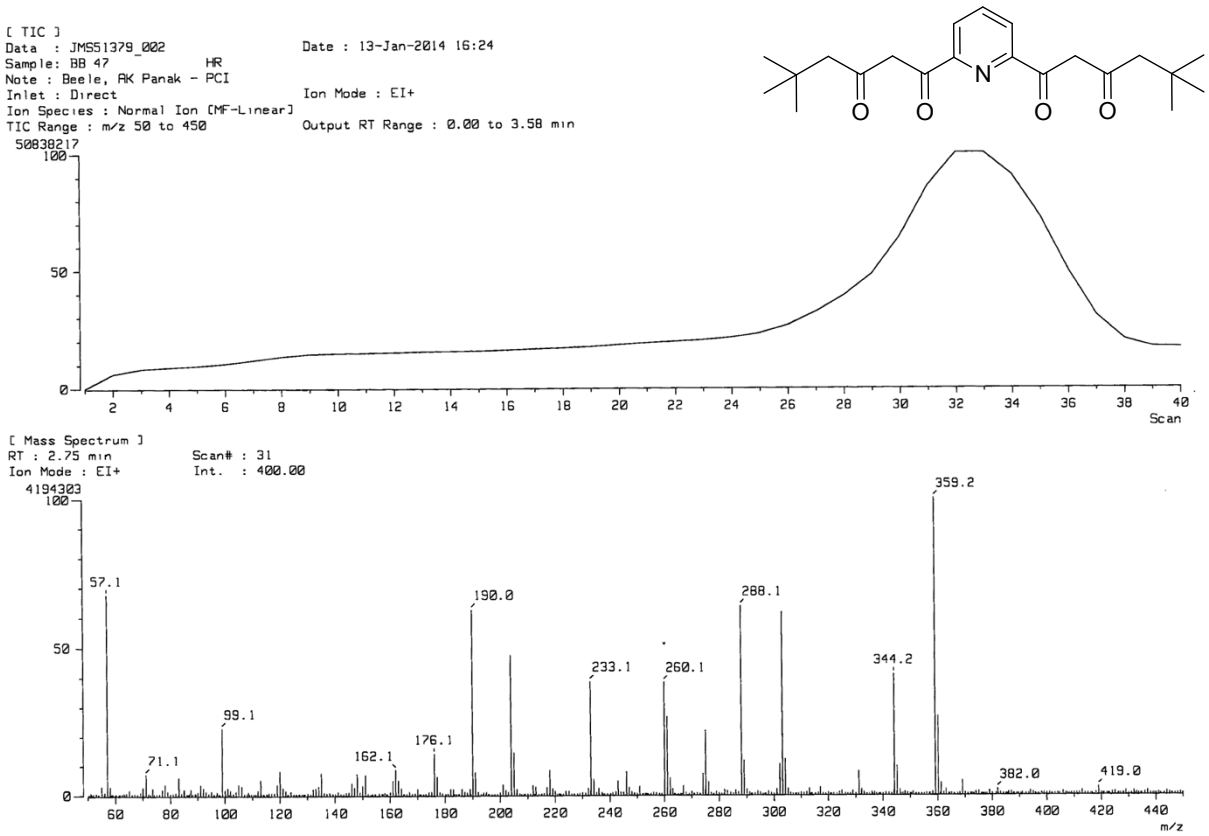

Figure S1: MS (EI) of 1,1'-(pyridine-2,6-diyl)bis(5,5-dimethylhexane-1,3-dione), $[M]^+$ = 359.2.

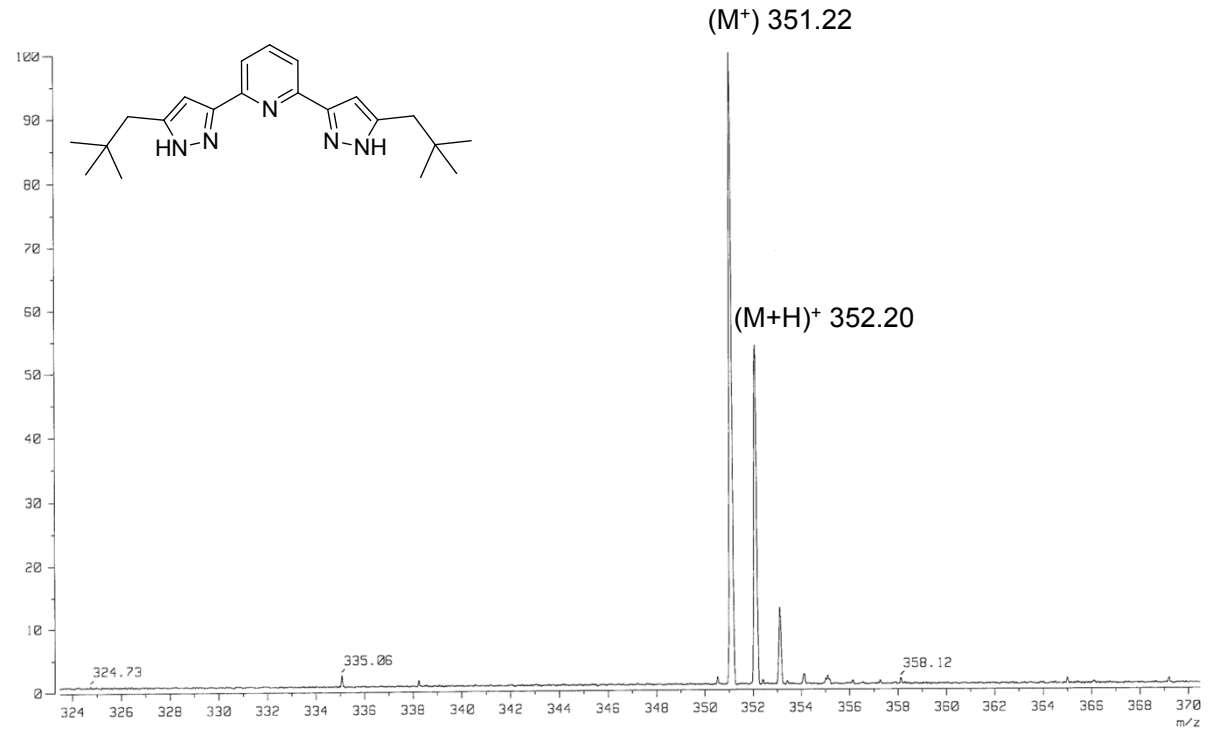

Figure S2: MS (LIFDI) of 2,6-bis(5-(2,2-dimethylpropyl)1H-pyrazol)-3-yl)-pyridine (C5-BPP) in CH_3OH, ion mode: FD+; detail m/z range 323.5 to 370.5; calculated for $C_{21}H_{30}N_5$ $[M+H]^+$ 352.25, found: 352.20; calculated for $C_{21}H_{29}N_5$ $[M]^+$: 351.24, found: 351.22.

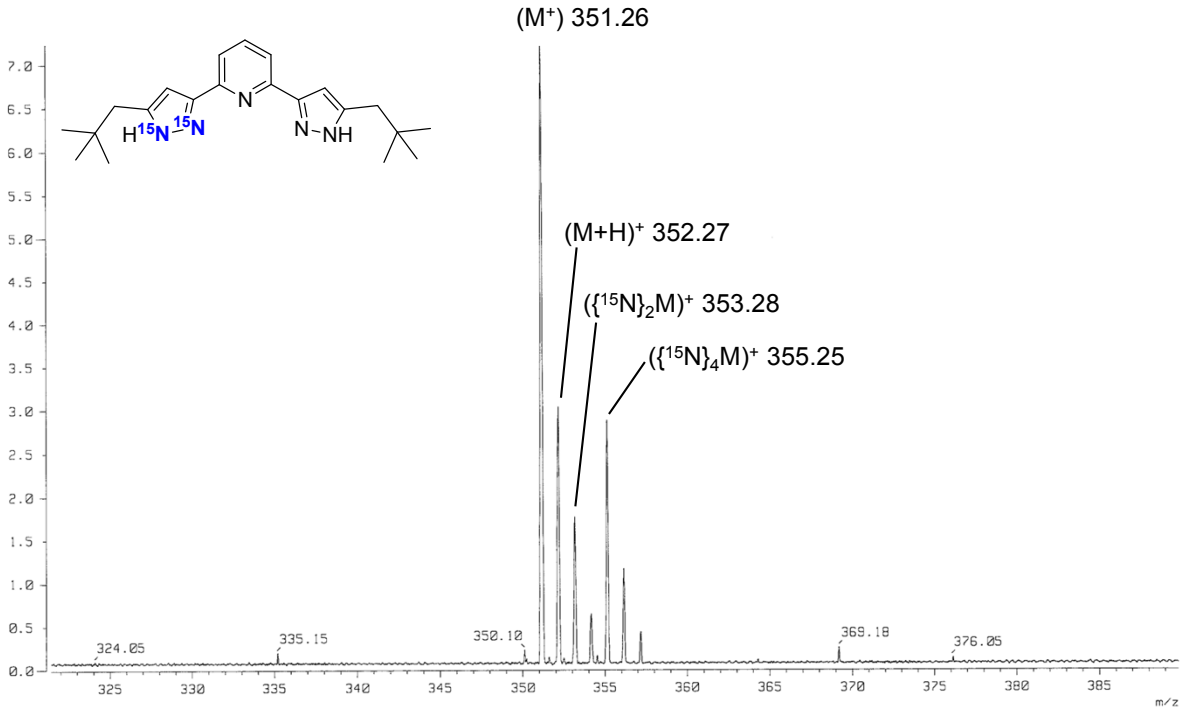

Figure S3: MS (LIFDI) of 2,6-bis(5-(2,2-dimethylpropyl)1H-pyrazol)-3-yl)-pyridine (C5-BPP) in CH_3OH, 10% ^{15}N-enrichment in pyrazole substituents; ion mode: FD+; detail m/z range 321.5 to 390; calculated for $C_{21}H_{29}N_3{}^{15}N_2$ $[M]^+$: 353.25, found: 353.28.

Analysis Info

Analysis Name	C:\Users\Public\Documents\MassSpek\Beele\icr18246_000001.d	Acquisition Date	07.11.2014 09:03:52
Method	ESI pos HPmix 200-1800	Instrument	ICR Apex-Qe
Sample Name	Y-C5BPP	Operator	I. Mitsch
Comment	Beele/Adam, AK Panak (PCI): Y-C5BPP in MeOH		

Acquisition Parameters

Accumulations	16	Collision Gas Flow Rate	0.5 L/sec	Capillary Entrance	4200.0 V
Broadband Low Mass	173.2 m/z	Collision Energy	0.5 eV	Calibration Date	Fri Sep 26 08:38:25 2014
Broadband High Mass	2500.0 m/z	Collision Cell RF	1200.0 V		
Data Acquisition Size	2097152	Q1 Resolution	5.0		
		Q1 Mass	200.000 m/z		

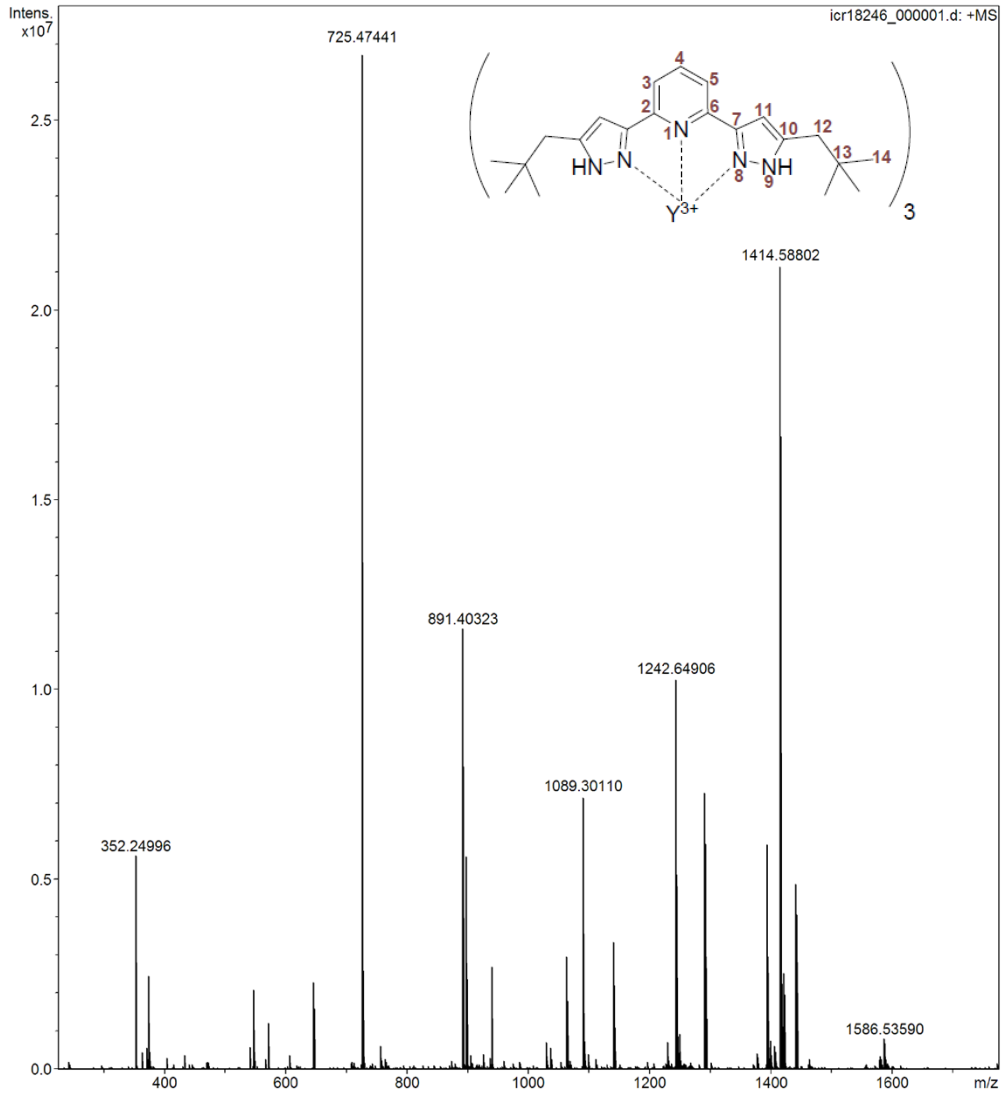

Figure S4: MS (ESI) of $[Y(C5\text{-}BPP)_3](OTf)_3$ in CH_3OH, pos. ion mode; m/z range 173.2 - 2500.0.

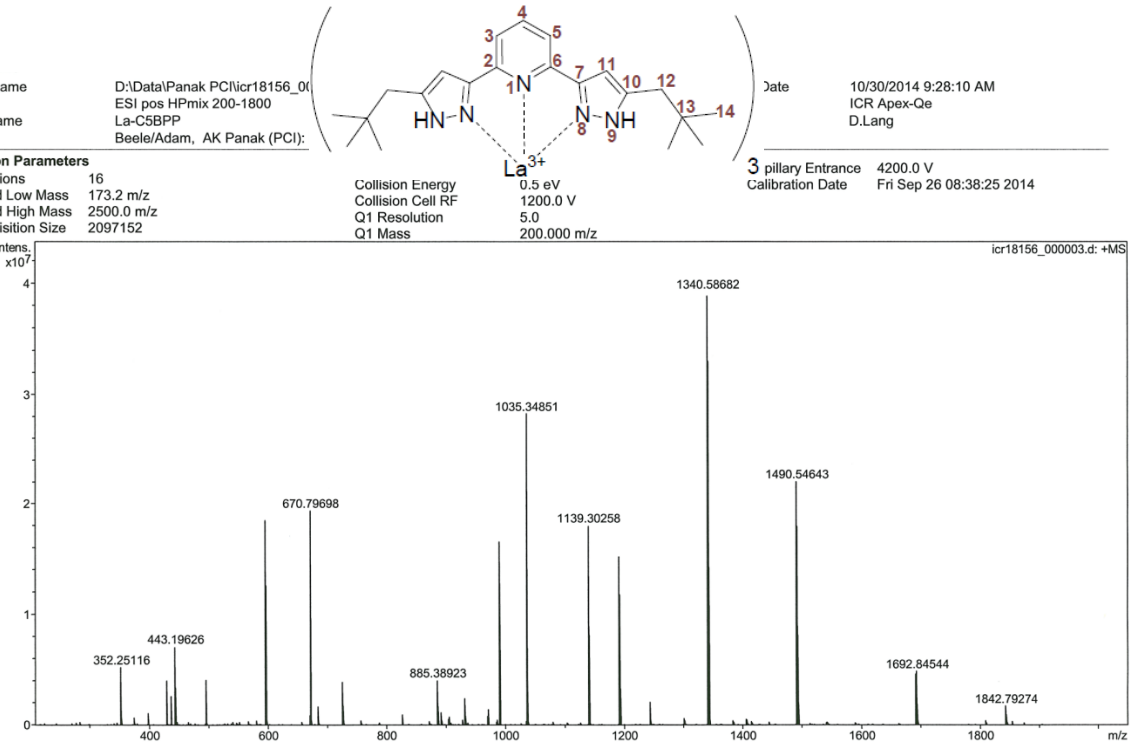

Figure S5: MS (ESI) of $[La(C5\text{-}BPP)_3](OTf)_3$ in CH_3OH, pos. ion mode; m/z range 173.2 - 2500.0.

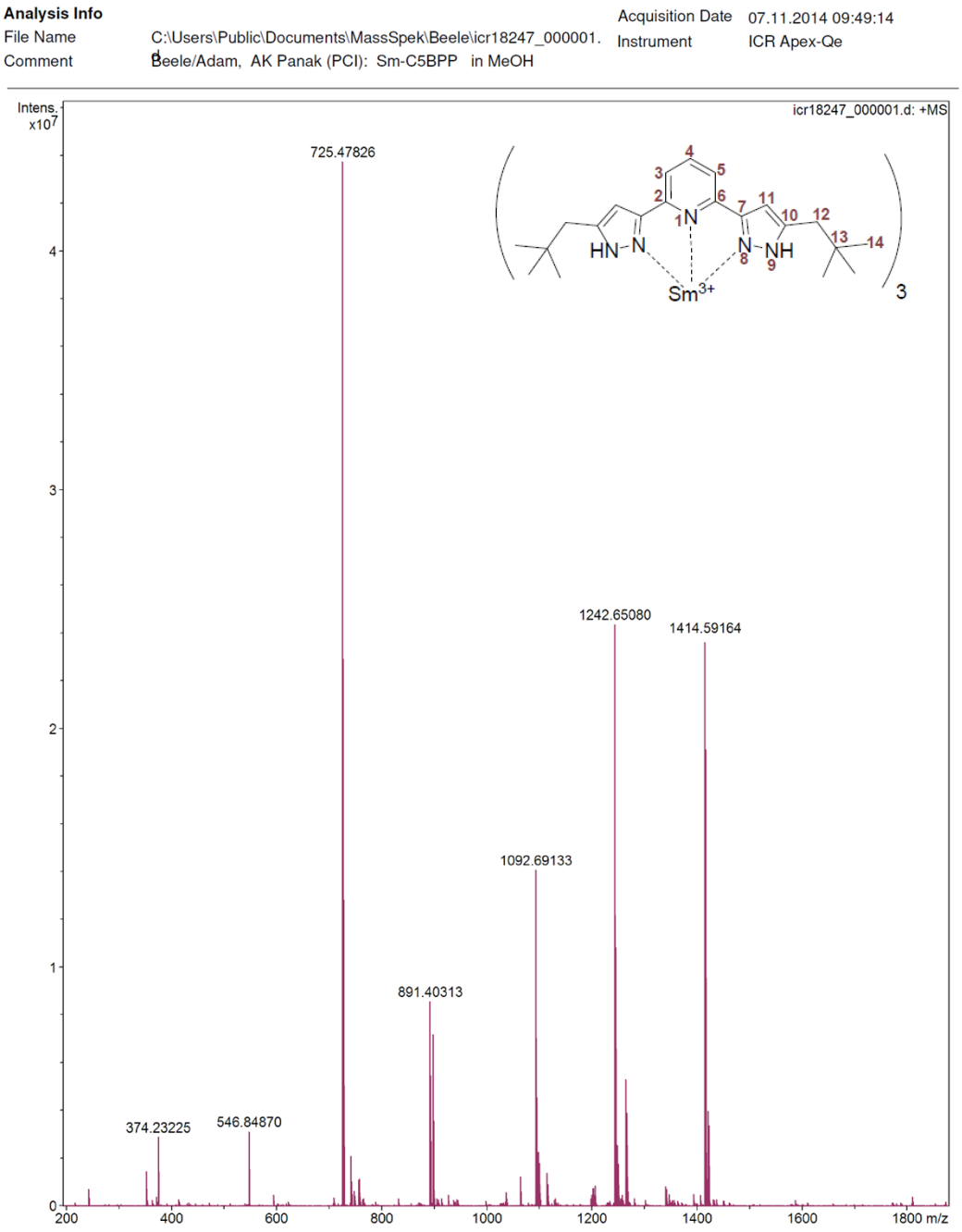

Figure S6: MS (ESI) of [Sm (C5-BPP)$_3$](OTf)$_3$ in CH_3OH, pos. ion mode; m/z range 173.2 - 2500.0.

Analysis Info

Analysis Name	C:\Users\Public\Documents\MassSpek\Beele\icr18248_000001.d	Acquisition Date	07.11.2014 10:08:49
Method	ESI pos HPmix 200-1800	Instrument	ICR Apex-Qe
Sample Name	Yb-C5BPP	Operator	I. Mitsch
Comment	Beele/Adam, AK Panak (PCI): Yb-C5BPP in MeOH		

Acquisition Parameters

Accumulations	16	Collision Gas Flow Rate	0.5 L/sec	Capillary Entrance	4200.0 V
Broadband Low Mass	173.2 m/z	Collision Energy	0.5 eV	Calibration Date	Fri Sep 26 08:38:25 2014
Broadband High Mass	2500.0 m/z	Collision Cell RF	1200.0 V		
Data Acquisition Size	2097152	Q1 Resolution	5.0		
		Q1 Mass	200.000 m/z		

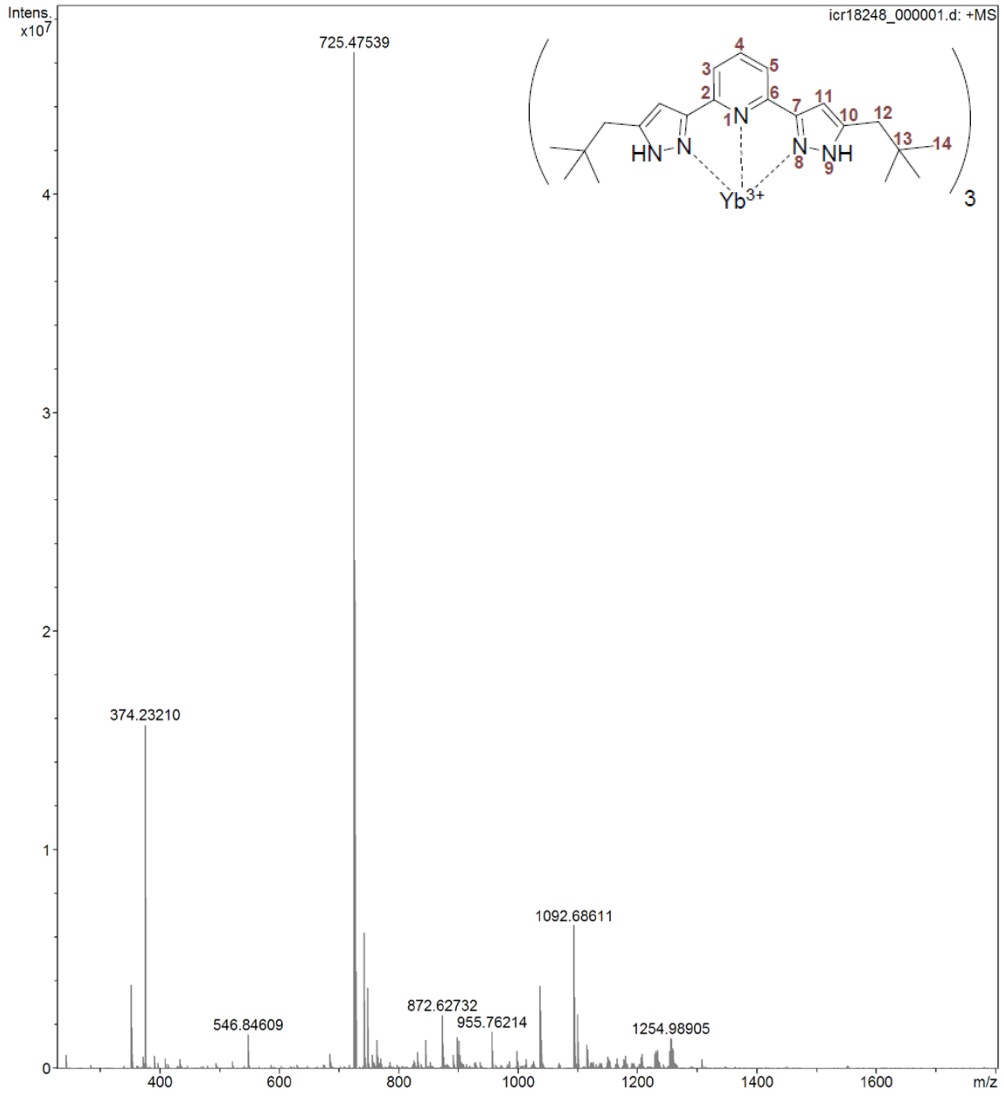

Figure S7: MS (ESI) of $[Yb(C5\text{-}BPP)_3](OTf)_3$ in CH_3OH, pos. ion mode; m/z range 173.2 - 2500.0.

Analysis Info

Analysis Name	C:\Users\Public\Documents\MassSpek\Beele\icr18249_000001.d	Acquisition Date	07.11.2014 10:18:54
Method	ESI pos HPmix 200-1800	Instrument	ICR Apex-Qe
Sample Name	Lu-C5BPP	Operator	I. Mitsch
Comment	Beele/Adam, AK Panak (PCI): Lu-C5BPP in MeOH		

Acquisition Parameters

Accumulations	16	Collision Gas Flow Rate	0.5 L/sec	Capillary Entrance	4200.0 V
Broadband Low Mass	173.2 m/z	Collision Energy	0.5 eV	Calibration Date	Fri Sep 26 08:38:25 2014
Broadband High Mass	2500.0 m/z	Collision Cell RF	1200.0 V		
Data Acquisition Size	2097152	Q1 Resolution	5.0		
		Q1 Mass	200.000 m/z		

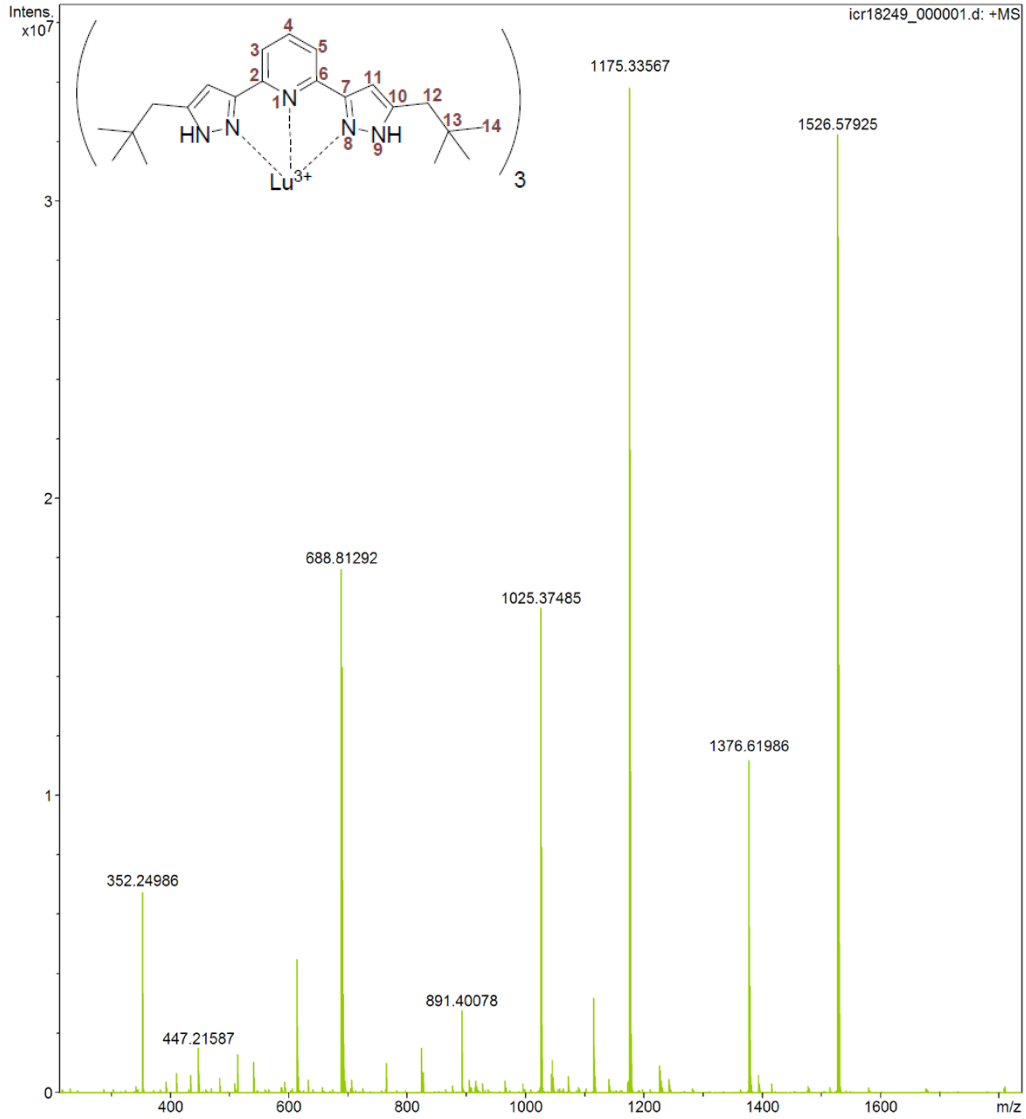

Figure S8: MS (ESI) of $[Lu(C5\text{-}BPP)_3](OTf)_3$ in CH_3OH, pos. ion mode; m/z range 173.2 - 2500.0.

NMR Spectra of $[^{243}Am(\{^{15}N\}C5\text{-}BPP)_3](OTf)_3$

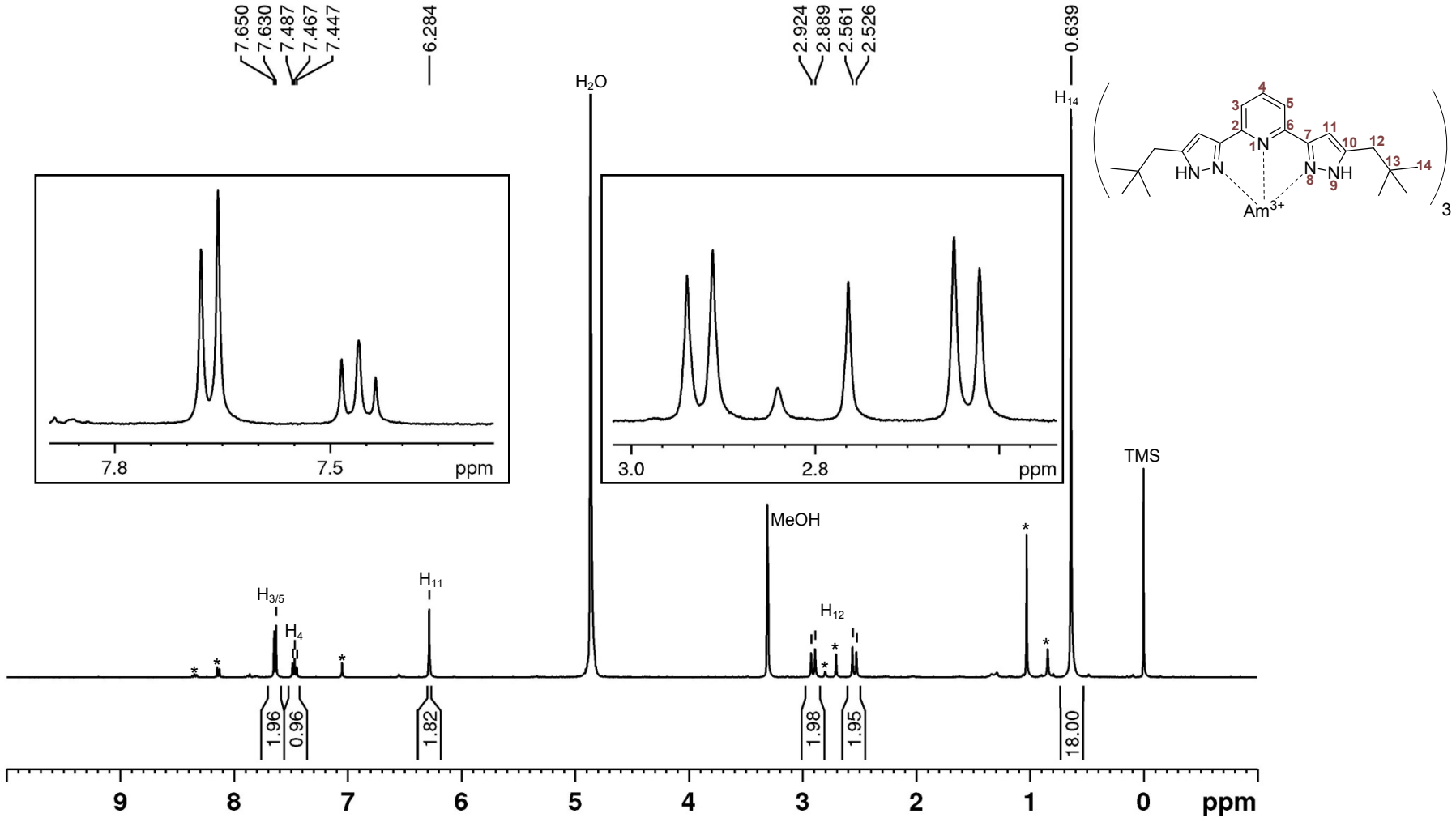

Figure S9: ^{1}H direct excitation spectrum of $[Am(\{^{15}N\}C5\text{-}BPP)_3](OTf)_3$. Signals labeled with an asterisk (*) belong to minor complex species.

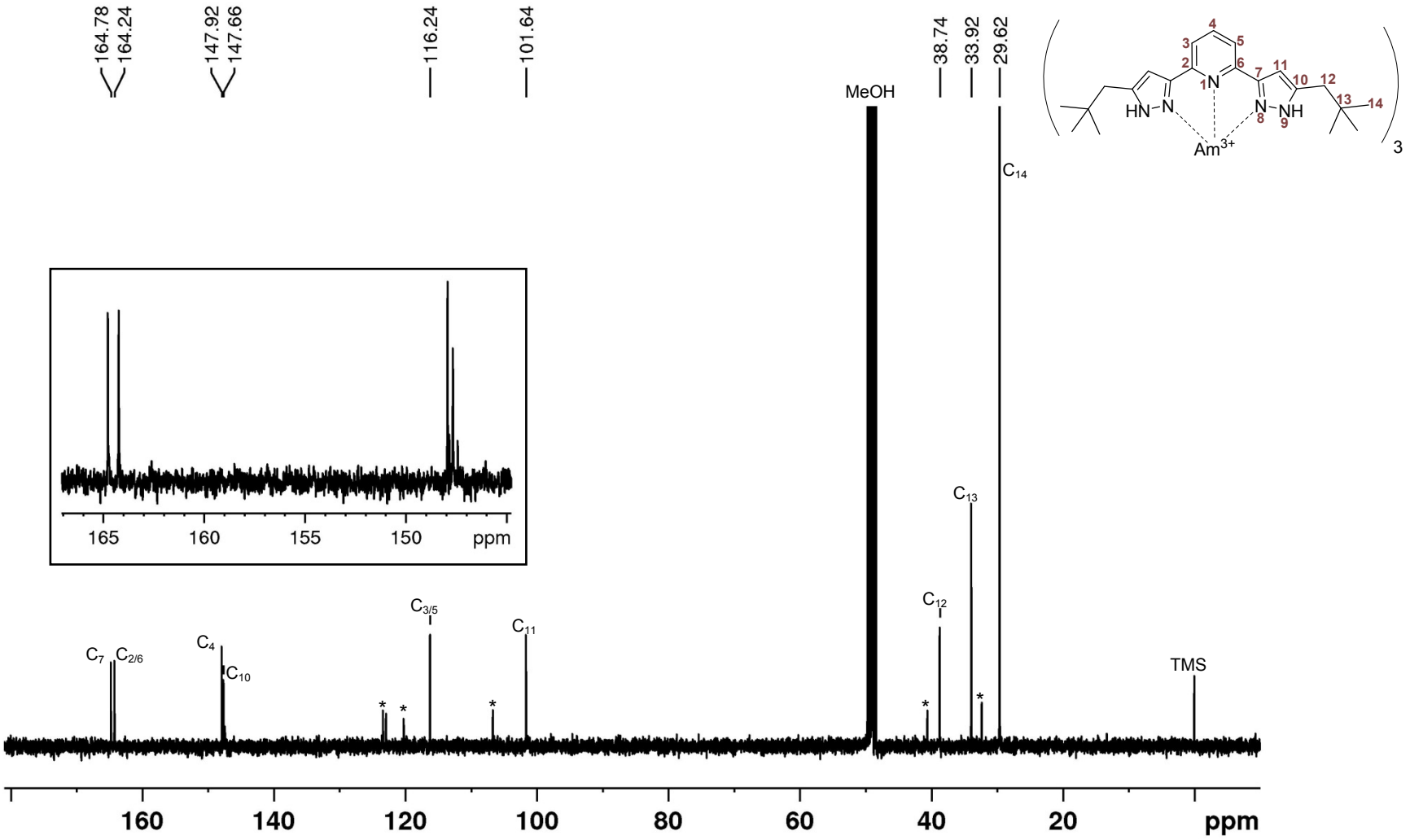

Figure S10: $\{^{1}H\}^{13}C$ direct excitation spectrum of $[Am(\{^{15}N\}C5\text{-}BPP)_3](OTf)_3$. Signals labeled with an asterisk (*) belong to minor complex species.

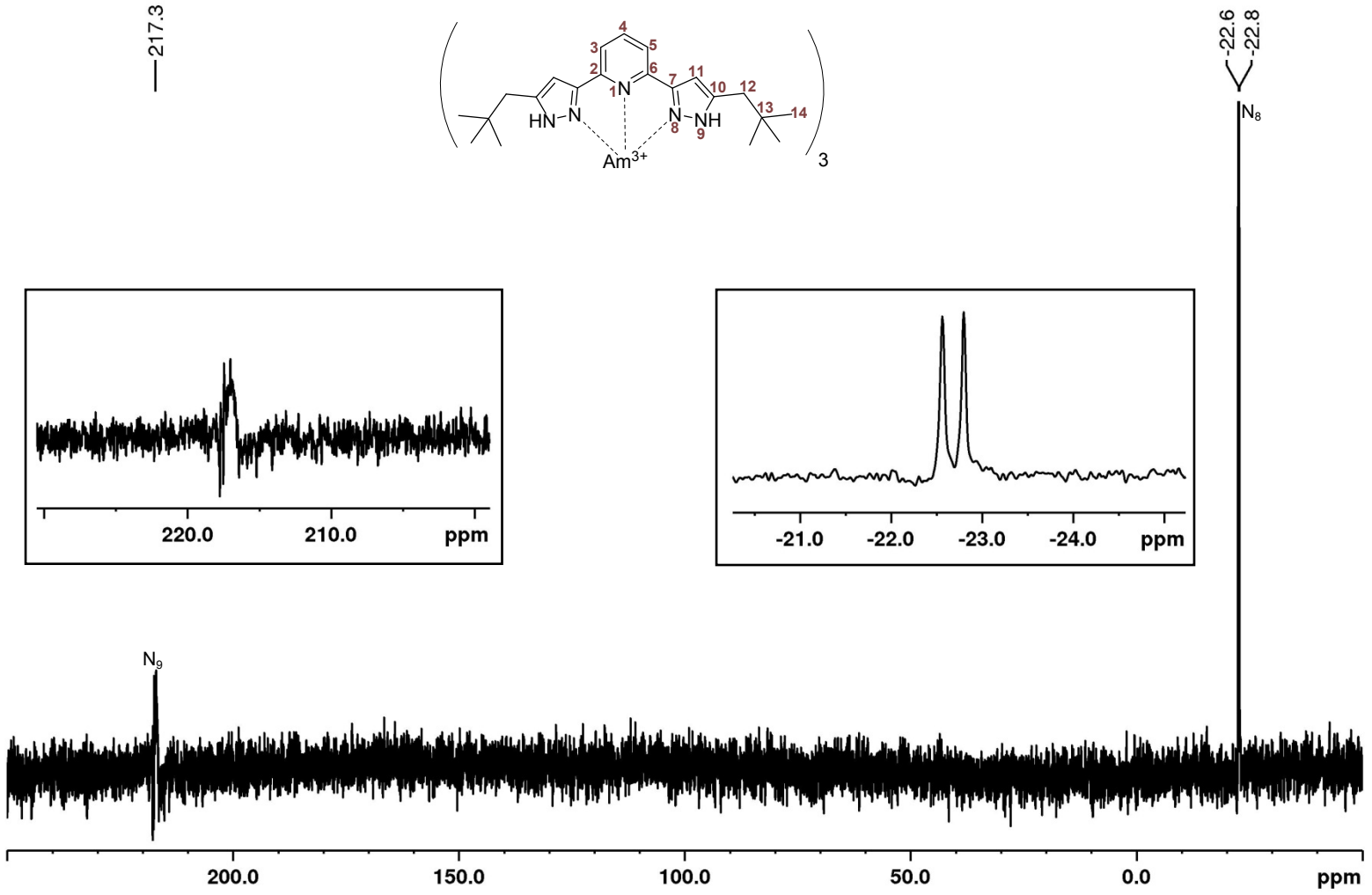

Figure S11: {^{1}H}^{15}N direct excitation spectrum of [Am({^{15}N}C5-BPP)$_3$](OTf)$_3$. To avoid negative NOEs inverse-gated decoupling was used.

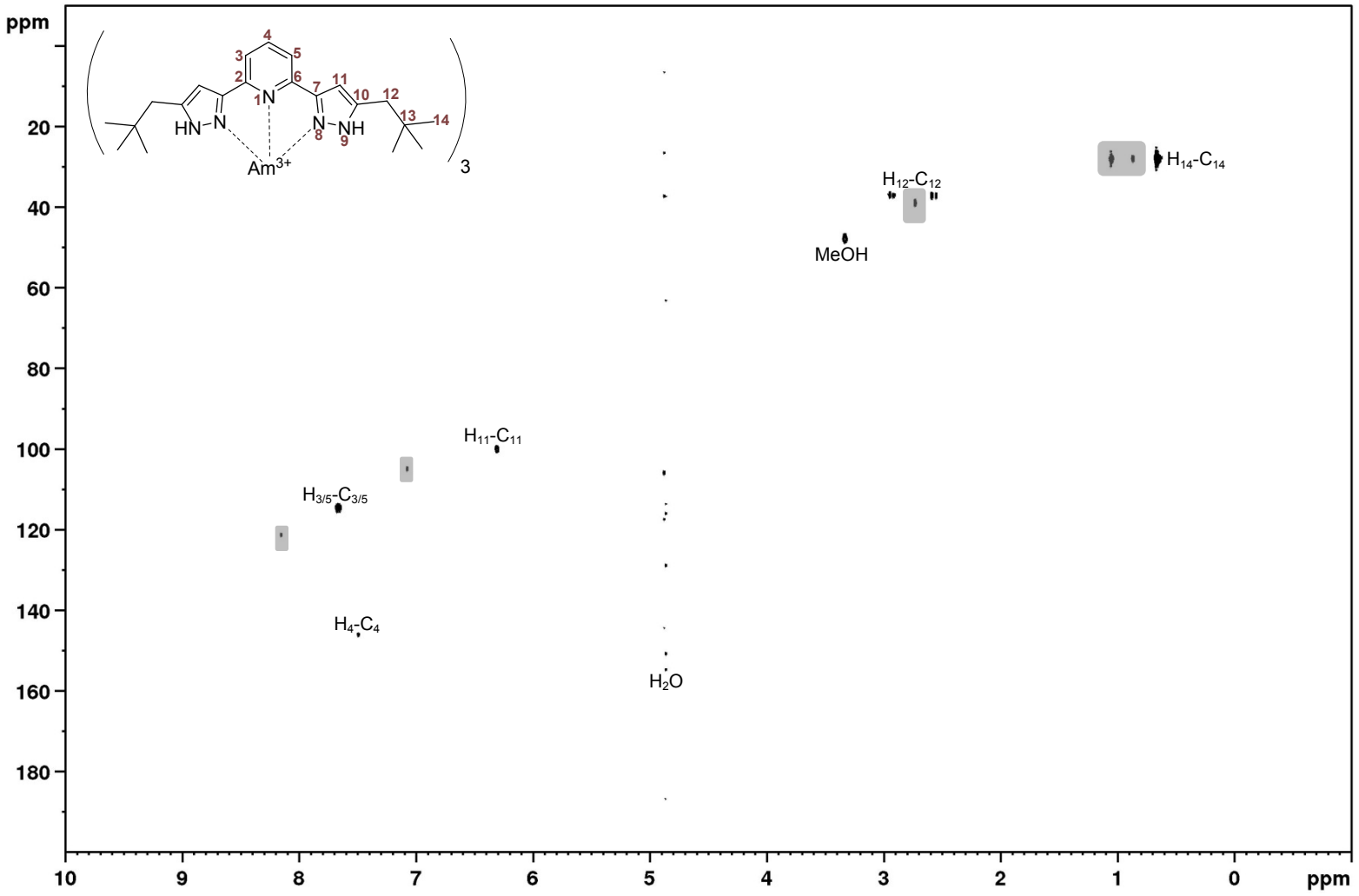

Figure S12: $^{1}H,^{13}C$-gHSQC spectrum of [Am({^{15}N}C5-BPP)$_3$](OTf)$_3$. 256 increments were sampled (8 scans) in the F1 direction, followed by linear prediction to 512 increments and zero-filling to 1k data points. Correlation signals belonging to minor complex species are shaded in gray.

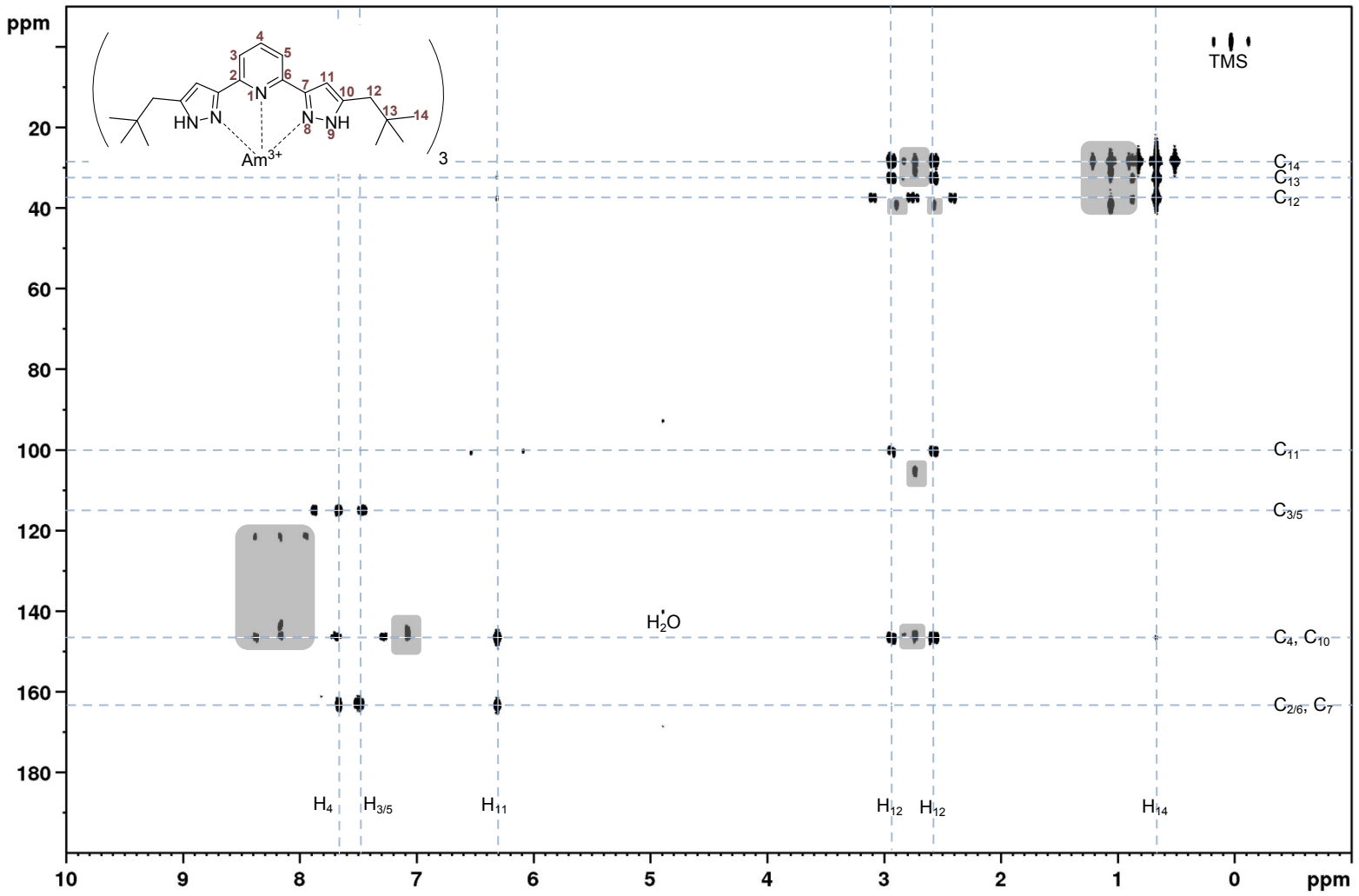

Figure S13: $^{1}H,^{13}C$-gHMBC spectrum of [Am({^{15}N}C5-BPP)$_3$](OTf)$_3$. 128 increments were sampled (32 scans) in the F1 direction, followed by linear prediction to 256 increments and zero-filling to 512 data points. Correlation signals belonging to minor complex species are shaded in gray.

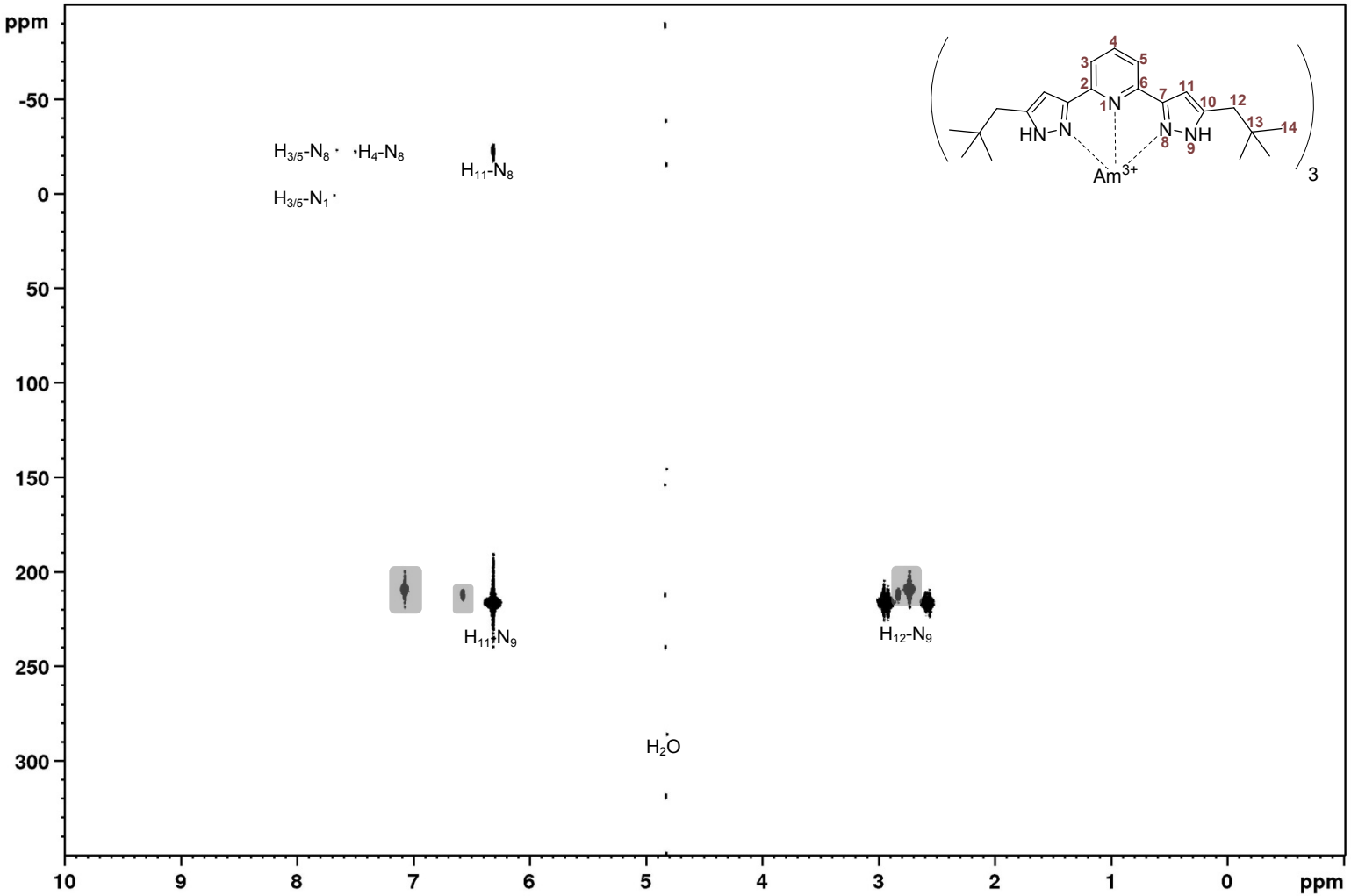

Figure S14: $^{1}H,^{15}N$-gHMQC spectrum of [Am({^{15}N}C5-BPP)$_3$](OTf)$_3$. 128 increments were sampled (128 scans) in the F1 direction, followed by linear prediction to 256 increments and zero-filling to 512 data points. Correlation signals belonging to minor complex species are shaded in gray.

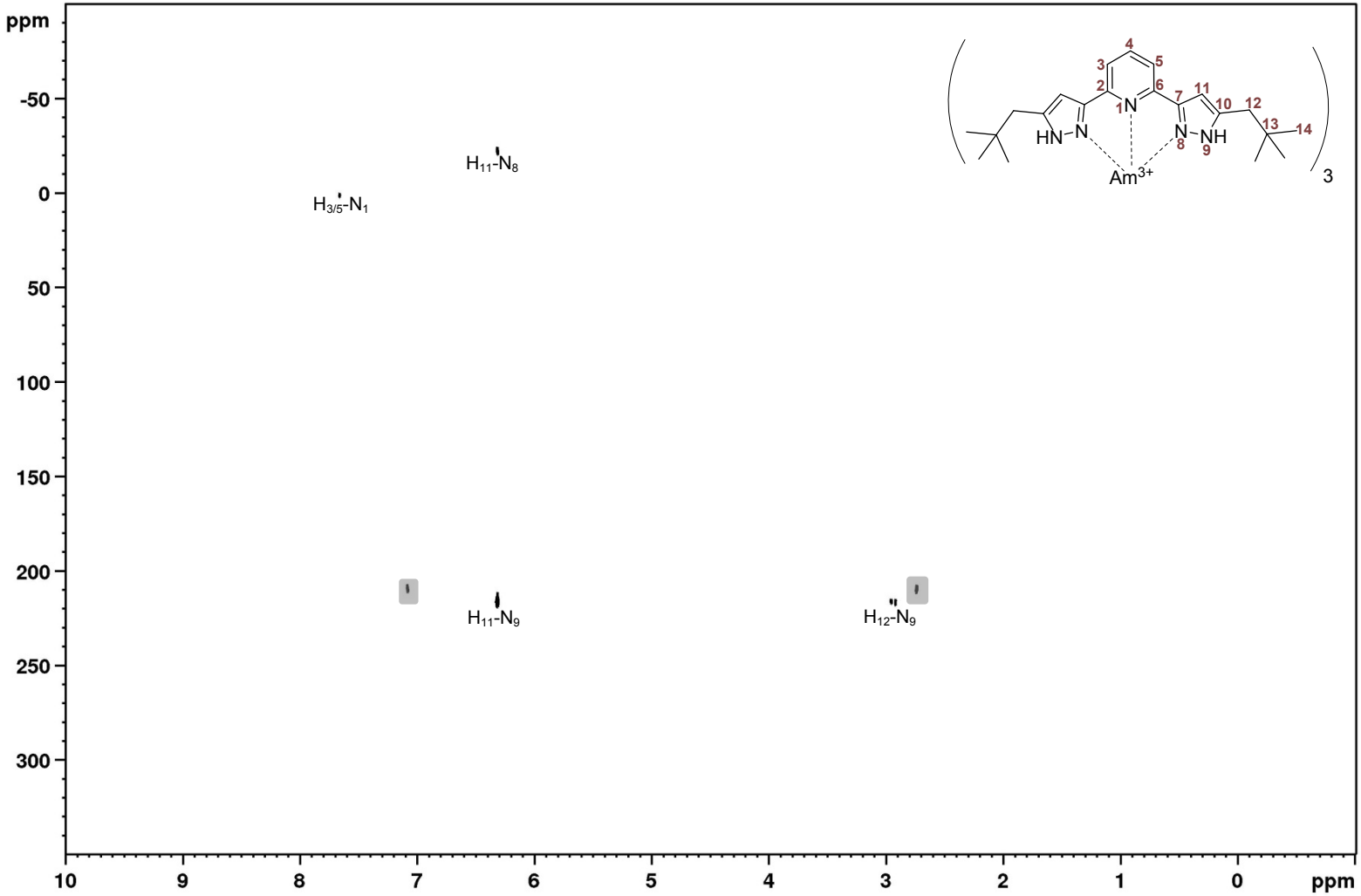

Figure S15: $^{1}H,^{15}N$-gHMQC spectrum of the unlabeled $[Am(C5\text{-}BPP)_3](OTf)_3$. 128 increments were sampled (128 scans) in the F1 direction, followed by linear prediction to 256 increments and zero-filling to 512 data points. Correlation signals belonging to minor complex species are shaded in gray.

Temperature-dependent ^{15}N NMR Spectra

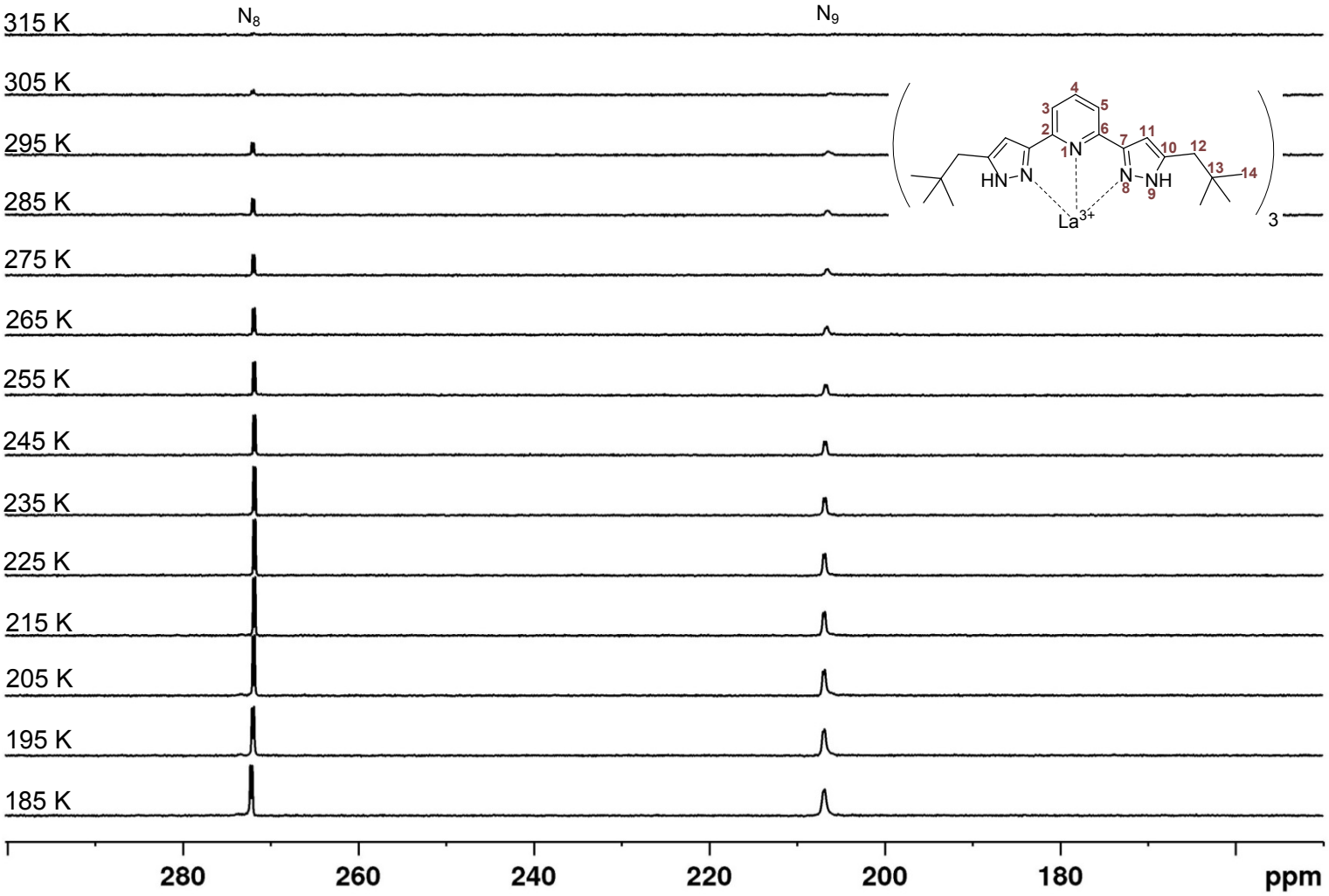

Figure S16: ^{15}N direct excitation spectra of [La({^{15}N}C5-BPP)$_3$](OTf)$_3$ in MeOD-d$_4$ at increasing temperatures (N_9 left side, N_8 right side). All spectra are referenced to the internal standard TMS by the lock signal.

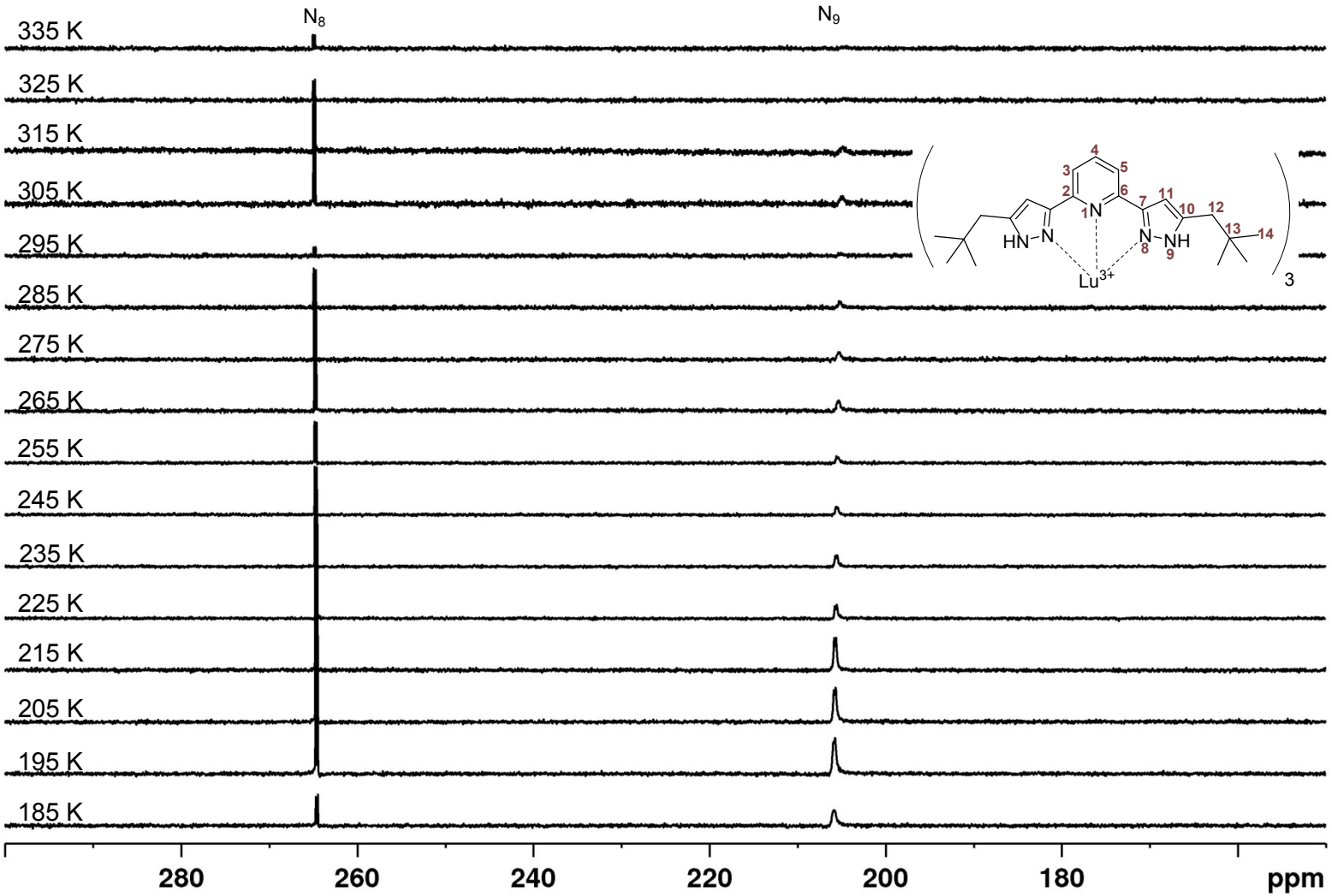

Figure S17: ^{15}N direct excitation spectra of [Lu({^{15}N}C5-BPP)$_3$](OTf)$_3$ in MeOD-d$_4$ at increasing temperatures (N_9 left side, N_8 right side). All spectra are referenced to the internal standard TMS by the lock signal.

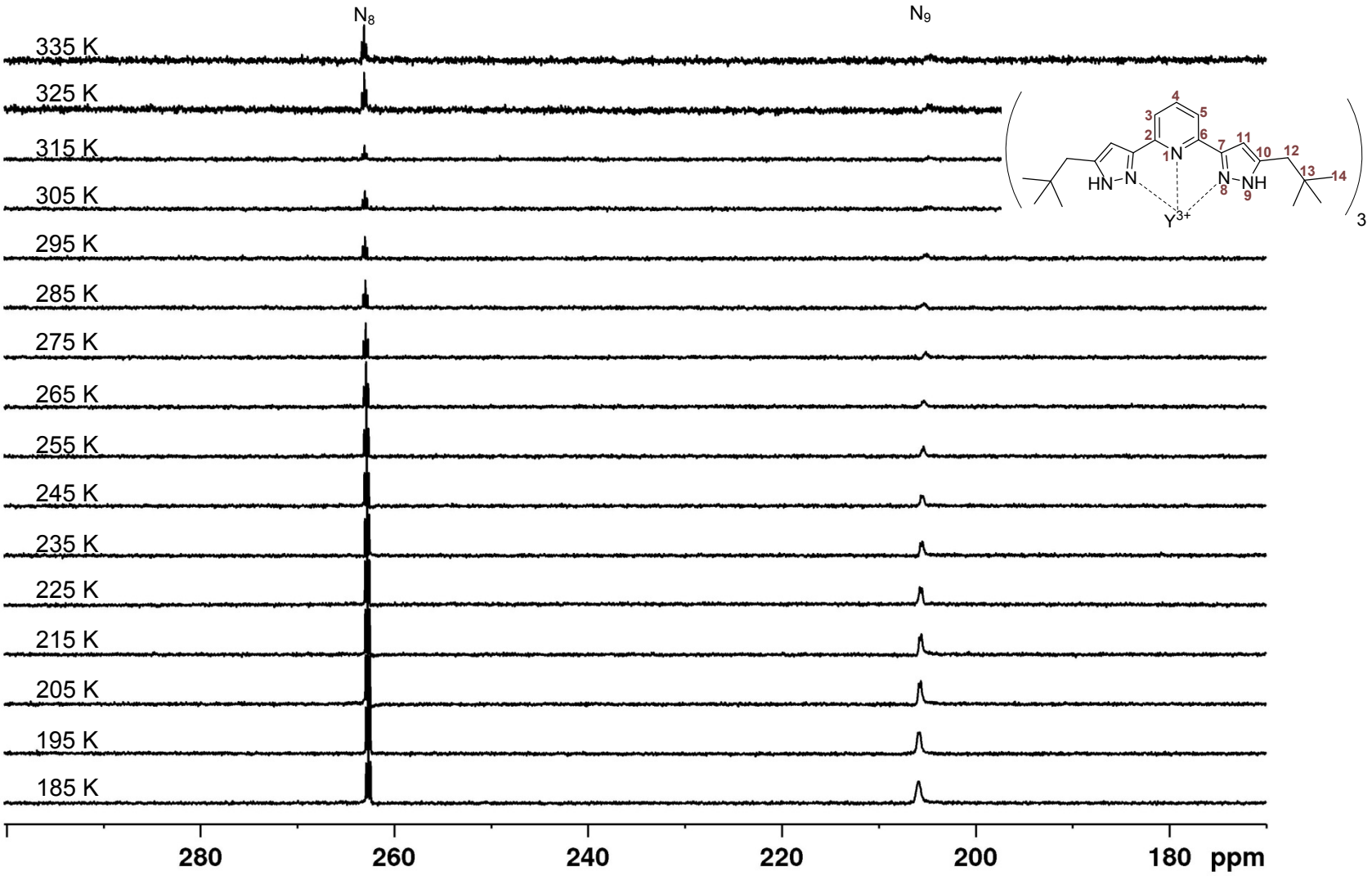

Figure S18: ^{15}N direct excitation spectra of [Y({^{15}N}C5-BPP)$_3$](OTf)$_3$ in MeOD-d$_4$ at increasing temperatures (N_9 left side, N_8 right side). All spectra are referenced to the internal standard TMS by the lock signal.

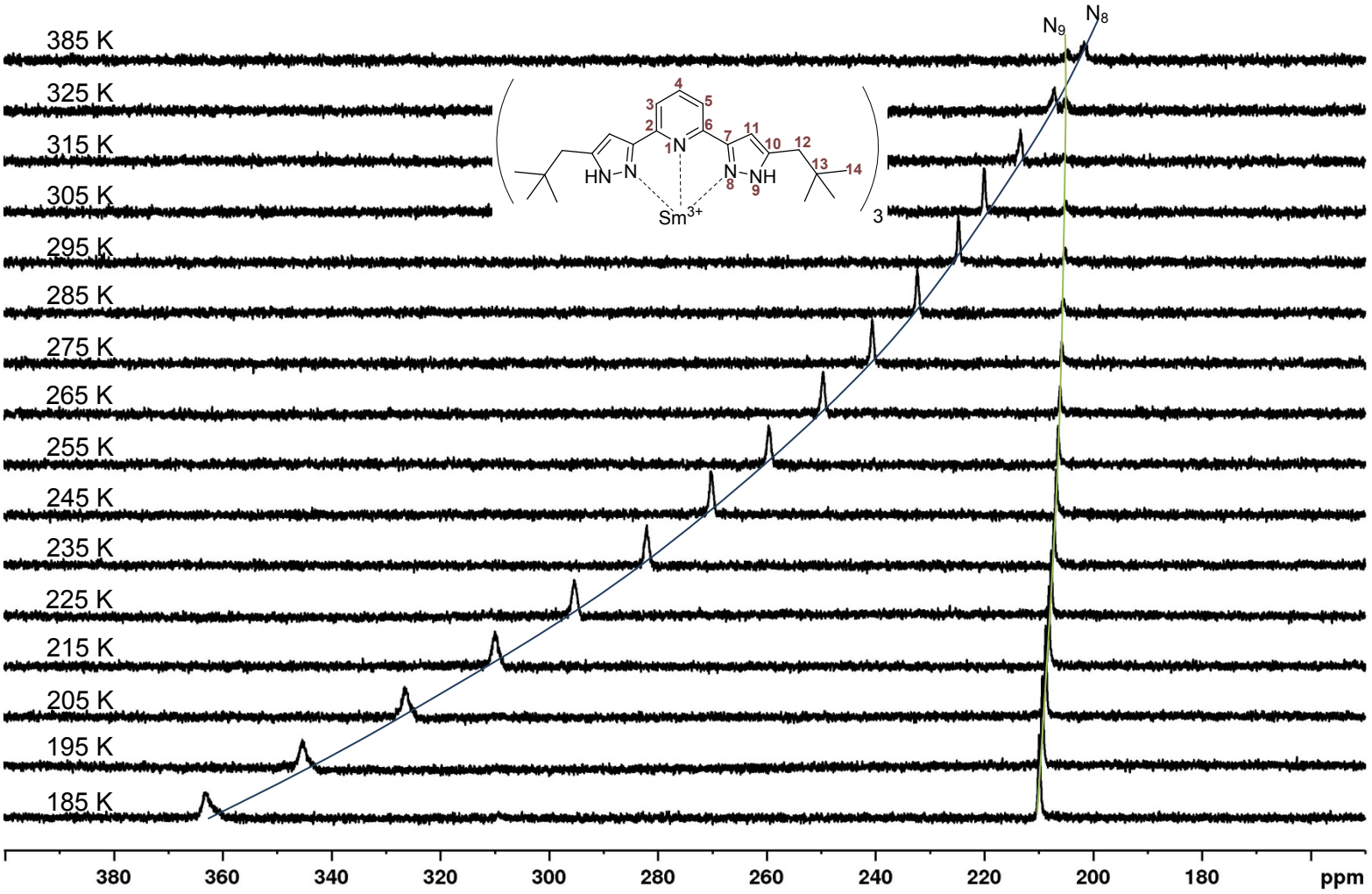

Figure S19: ^{15}N direct excitation spectra of [Sm({^{15}N}C5-BPP)$_3$](OTf)$_3$ in MeOD-d$_4$ at increasing temperatures (N_9 left side, N_8 right side). All spectra are referenced to the internal standard TMS by the lock signal.

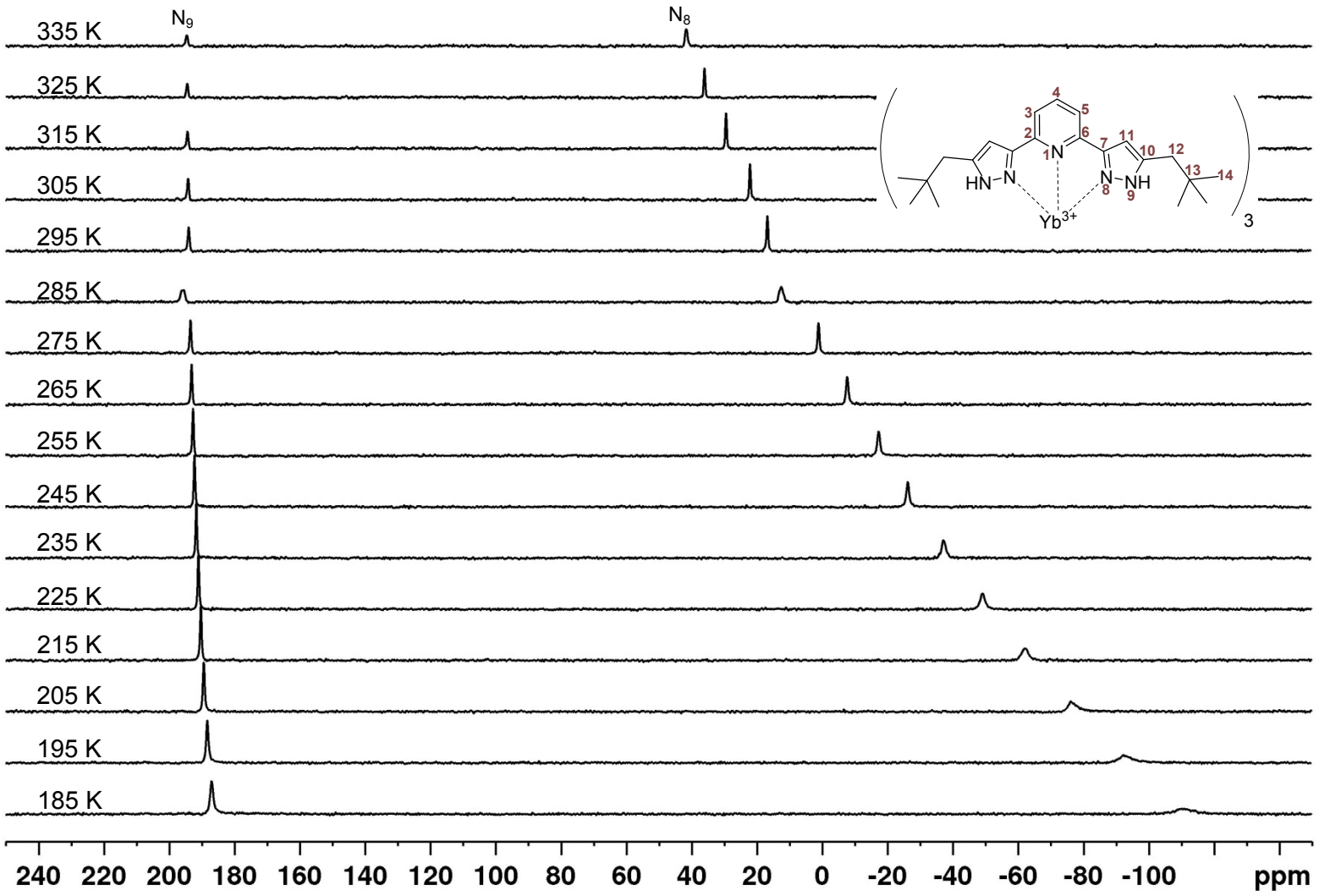

Figure S20: ^{15}N direct excitation spectra of [Yb({^{15}N}C5-BPP)$_3$](OTf)$_3$ in MeOD-d$_4$ at increasing temperatures (N_9 left side, N_8 right side). All spectra are referenced to the internal standard TMS by the lock signal.

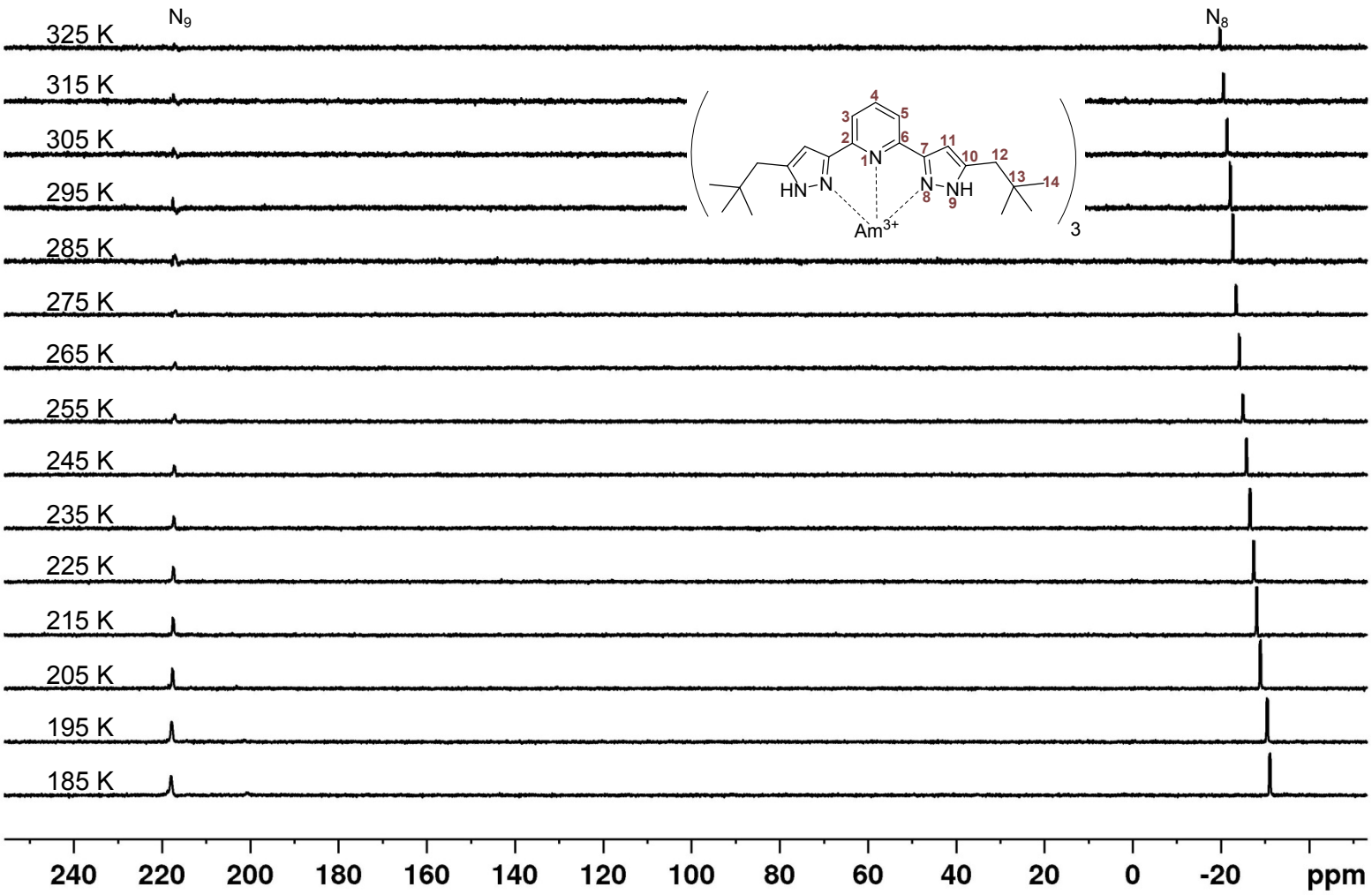

Figure S21: ^{15}N direct excitation spectra of [Am({^{15}N}C5-BPP)$_3$](OTf)$_3$ in MeOD-d$_4$ at increasing temperatures (N_9 left side, N_8 right side). All spectra are referenced to the internal standard TMS by the lock signal.